International Journal of Mechanical and Production Engineering Research and Development (IJMPERD)
ISSN (P): 2249–6890; ISSN (E): 2249–8001
Vol. 10, Issue 2, Apr 2020, 1147–1156

INFLUENCE OF ASPECT RATIO AND THERMOMECHANICAL ENVIRONMENT ON THE GRADED FGM PLATES

MANISH BHANDARI

Assistant Professor, Department of Mechanical Engineering, MBM Engineering. College, JNV University, Jodhpur, Rajasthan, India

ABSTRACT

The Functionally Graded Material (FGM) are combination of ceramic and metal and hence exhibit properties such that FGM becomes suitable for the conditions where high temperature environment is prevailing. The combination of the FGM is governed by the material variation which is done by following certain laws of material distribution such as Power law, Sigmoid law, Exponential law etc. The analysis of FGM under thermal and thermo-mechanical of FGM structures is one important dimension which has drawn attention of scientists in the past few years. Thermal and thermo mechanical environment have a big impact on the bending response of FGM plate. Various material gradient functions play a great role in the performance of FGM. In the current work, the FGM plate is modelled using Finite element method and non dimensional deflection, stress and strain are calculated with the application of three FGM material gradation laws namely Power-law, Sigmoid and Exponential law functions. The results are compared for various values of volume fraction index.

KEYWORDS: FGM, Deflection, Stress, Strain & Thermo-Mechanical

Received: Mar 03, 2020; **Accepted:** Mar 23, 2020; **Published:** Apr 06, 2020; **Paper Id.:** IJMPERDAPR2020111

Original Article

1. INTRODUCTION

The graded combination of ceramic and metal are called Functionally Graded Material (FGM) and hence show properties in such a manner that FGM becomes appropriate for the circumstances where high thermal conditions are prevailed. The properties of the FGM are governed by the volume of the material fraction which is performed by following distribution laws such as Power law distribution, Sigmoid law distribution, Exponential law distribution etc. The performance analysis of FGM under mechanical and thermal loading of FGM structures is one prominent direction which has attracted attention of scientists. Power-law distribution function (P-FGM) has been used by Woo [1]and Reddy [2], Sigmoid law distribution function (S-FGM) has been considered by Hui [3].Sigmoid law distribution function used two power law distributions simultaneously and hence provide smoother material volume distribution as compared to Power law distribution to the layered FGM. While using Exponential law the material properties estimated are intermediate to those which are calculated using Power-law distribution function (n=0.5) and Power-law distribution function (n=2). Duc [4] derived analytical solution in close form of a linear thermo elastic elliptic plate rigidly fixed at the mid-plane. The FGMs are sensitive to the heat flow variation in or out of the structure, as compared to that of the isotropic material structures. Xiaohui [5] concluded that the thermal field and the material gradient have significant effect on thermo-mechanical behavior of the FGM plates. They considered lateral strain and computed that the additional deformation parameters do not increase when transverse normal strain includes the thermal expansion coefficient and thermal loading.

Thermal and thermo mechanical environment have a big impact on the bending response of FGM plate. Various material gradient functions play a great role in the performance of FGM. In the current work, the FGM plate is modelled using Finite element method and non dimensional deflection, stress and strain are calculated with the application of three FGM material gradation laws namely Power-law, Sigmoid and Exponential law functions. The results are compared for various values of volume fraction index.

2. METHODOLOGY

Thermal and thermo-mechanical analysis is performed for FGM plate made of Aluminum (Al) –Zirconia (ZrO_2). The boundary condition for plate which is used here is simply supported at all of its edges. The thickness of the plate (h) is taken 0.02m. The aspect ratio (a/b) is defined as the ratio of plate side lengths.

2.1 Thermal Analysis

Thermal analysis is performed by providing thermal environment to the FGM plate. Temperature of 100 °C is applied at ceramic top surface while metal surface and all edges are maintained at a temperature of 0 °C.

2.2 Thermomechanical Analysis

Thermomechanical analysis is performed by providing thermal environment to the FGM plate alongwith a mechanical udl (p_o) of 1 MPa. Temperature of 100 °C is applied at ceramic top surface while metal surface and all edges **are** maintained at a temperature of 0 °C.

The analysis is performed for various values of the volume fraction exponent (n) in Power law-FGM, Sigmoid law-FGM and Exponential law-FGM e.g. for pure ceramic (n=0), pure metal (n=∞), P-FGM (n=2), P-FGM (n=0.5), S-FGM (n=2), S-FGM (n=0.5) and E-FGM. The results discussed in non-dimensional parametric form i.e. non-dimensional deflection ($=u_z/h$), non-dimensional tensile stress ($=\sigma_x/p_o$), non-dimensional shear stress ($\bar{c}=\sigma_{xy}/p_o$), Strain(e_x) and Shear strain (e_{xy}) where 'u_z' is deflection, 'σ' is stress. Finite element method has been used to model the FGM plate in ANSYS.

3. RESULTS

3.1 Effect of Aspect Ratio (a/b) in Constant Thermal Environment

Non dimensional parameters are computed when the FGM plate is subjected to constant thermal environment of 100 °C for various values of aspect ratio (a/b). Non dimensional parameters are depicted in tables 1,2,3,4 and 5. Graphical comparisons have presented in figure 1, 2,3,4 and 5.

The observations are as follows:

- Maximum deflection for P-FGM-n2 ($\overline{u_z}$ = 0.55) is found to be greater than that of S-FGM-n2 ($\overline{u_z}$ =0.35). Also deflection for P-FGM-n0.5 ($\overline{u_z}$ = 0.4) is found to be more than that of S-FGM-n0.5 ($\overline{u_z}$ =0.24) (table 1). The deflection shows increase up to aspect ratio 2 and constant nature afterwards (figure 1).
- Maximum tensile stress for P-FGM-n2 ($\overline{\sigma_x}$ = 43.3) is found to be greater than that of S-FGM-n2 ($\overline{\sigma_x}$=40.1). Also tensile stress for P-FGM-n0.5 ($\overline{\sigma_x}$ = 27.9) is found to be less than that of S-FGM-n0.5 ($\overline{\sigma_x}$ =31.1) (table 2). The tensile stress is showing sharp rise up to aspect ratio 1 and decrease afterwards (figure 2).

- Maximum shear stress for P-FGM-n2 ($\overline{\sigma_{xy}}$ = 512) is found to be greater than that of S-FGM-n2 ($\overline{\sigma_{xy}}$=478). Also shear stress in case of P-FGM-n0.5 ($\overline{\sigma_{xy}}$ = 430) is found to be less than that of S-FGM-n0.5 ($\overline{\sigma_{xy}}$ =438) (table 3). The shear stress is showing sharp rise up to aspect ratio 1 and gradual decrease afterwards (figure 3).
- Maximum strain (ex) for P-FGM-n2 (ex = 1.09) is found to be greater than that of S-FGM-n2 (ex=1.01) (table 4). The strain is showing sharp decline up to aspect ratio 1 and sharp decline afterwards (figure 4)
- The maximum shear strain (exy) for P-FGM-n2 (exy = 18.04) is found to be greater than that of S-FGM-n2 (exy=17.7) (table 5). The shear strain is showing sharp rise up to aspect ratio 2 and gradual decline afterwards (figure 5).
- Maximum deflection for E-FGM ($\overline{u_z}$ = 0.51) lies in between P-FGM-n2 ($\overline{u_z}$ = 0.54) and P-FGM-n0.5 ($\overline{u_z}$ = 0.34). Similar trend is also observed in case of tensile stress, shear stress, strain and shear strain where the value of these parameters for E-FGM is found to be in between P-FGM n2 and P-FGM n0.5.

3.1.1 Non-Dimensional Deflection ($\overline{u_z}$)

Table 1: Non-Dimensional Deflection ($\overline{u_z}$) Under Constant Thermal Environment

a/b	a/h	Ceramic (n=0)	P-FGM-n 0.5	S-FGM-n 0.5	P-FGM-n2	S-FGM-n2	E-FGM	Metal (n=∞)
0.16	8	0.02	0.01	0.01	0.01	0.01	0.01	0.02
0.2	10	0.03	0.02	0.01	0.02	0.01	0.02	0.04
0.25	12.5	0.05	0.02	0.02	0.03	0.02	0.03	0.05
0.5	25	0.19	0.09	0.06	0.13	0.08	0.12	0.2
0.75	37.5	0.35	0.17	0.1	0.23	0.15	0.22	0.37
1	50	0.49	0.23	0.14	0.33	0.21	0.3	0.52
2	100	0.76	0.36	0.22	0.5	0.32	0.47	0.8
3	150	0.81	0.39	0.24	0.54	0.34	0.5	0.86
4	200	0.83	0.4	0.24	0.54	0.34	0.51	0.88
5	250	0.83	0.4	0.24	0.54	0.34	0.51	0.88

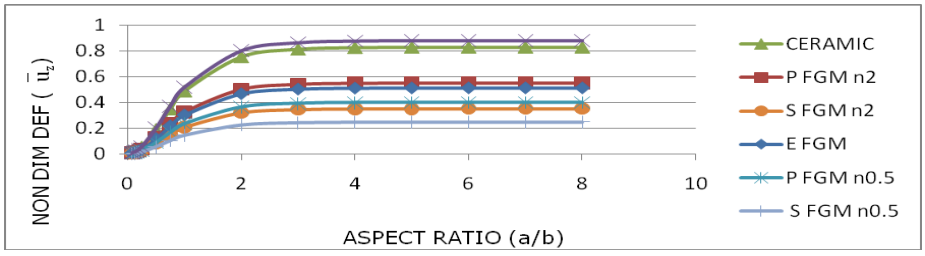

Figure 1: Non-Dimensional Deflection ($\overline{u_z}$) Under Constant Thermal Environment.

3.1.2 Non-Dimensional Tensile Stress ($\overline{\sigma_x}$)

Table 2: Non-Dimensional Tensile Stress ($\overline{\sigma_x}$) Under Constant Thermal Environment

a/b	a/h	Ceramic (n=0)	P-FGM-n 0.5	S-FGM-n 0.5	P-FGM-n2	S-FGM-n2	E-FGM	Metal (n=∞)
0.16	8	4.6	16	17.8	24.8	22.9	21.7	7.1
0.2	10	4.6	16	17.8	24.8	22.9	21.7	7.1
0.25	12.5	4.6	16	17.8	24.8	22.9	21.7	7.1
0.5	25	4.5	15.8	17.6	24.5	22.6	21.4	7
0.75	37.5	4.4	15.4	17.1	23.9	22.1	20.9	6.8

1	50	8	27.9	31.1	43.3	40.1	37.9	12.3
2	100	3.9	13.7	15.2	21.2	19.6	18.6	6
3	150	3.6	12.5	13.9	19.4	18	17	5.5
4	200	3.3	11.4	12.7	17.6	16.3	15.4	5
5	250	2.9	10.2	11.4	15.9	14.7	13.9	4.5

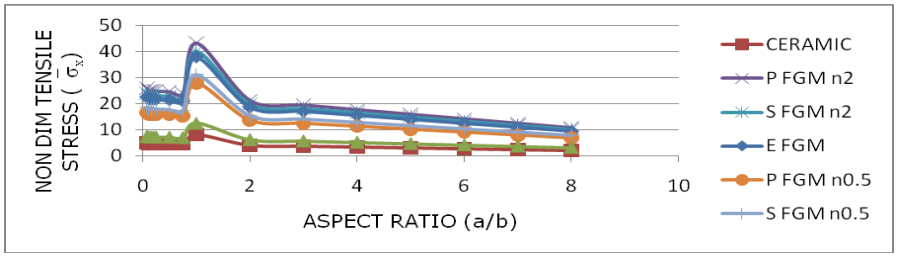

Figure 2: Non-Dimensional Tensile Stress ($\overline{\sigma_x}$) Under Constant Thermal Environment

3.1.3 Non-Dimensional Shear Stress ($\overline{\sigma_{xy}}$)

Table 3: Non-Dimensional Shear Stress ($\overline{\sigma_{xy}}$) under Constant Thermal Environment

a/b	a/h	Ceramic (n=0)	P-FGM-n 0.5	S-FGM-n 0.5	P-FGM-n2	S-FGM-n2	E-FGM	Metal (n=∞)
0.16	8	286	325	332	391	362	369	303
0.2	10	302	343	350	412	382	389	320
0.25	12.5	317	360	367	433	401	409	336
0.5	25	358	407	415	489	453	462	379
0.75	37.5	375	425	433	511	473	482	396
1	50	378	430	438	512	478	487	400
2	100	357	405	413	487	451	459	378
3	150	333	379	386	455	421	429	353
4	200	315	358	364	430	398	406	333
5	250	300	341	347	409	379	386	317

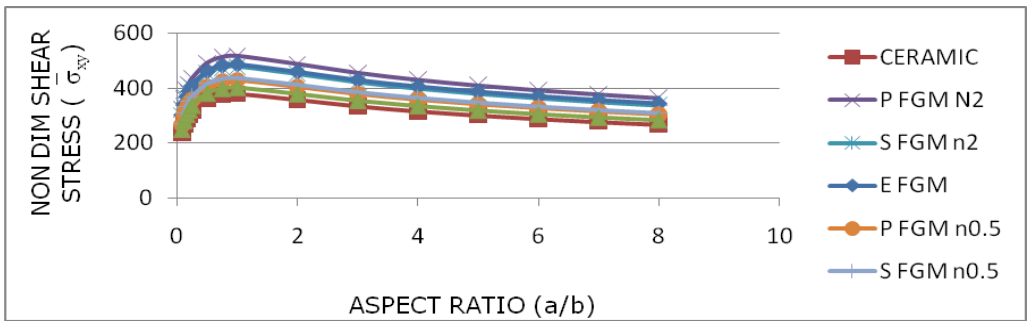

Figure 3: Non-Dimensional Shear Stress ($\overline{\sigma_{xy}}$) Under Constant Thermal Environment.

Strain (e_x)

Table 4: Strain (e_x x1000) Under Constant Thermal Environment

a/b	a/h	Ceramic (n=0)	P-FGM-n 0.5	S-FGM-n 0.5	P-FGM-n2	S-FGM-n2	E-FGM	Metal (n=∞)
0.16	8	1.63	0.46	0.86	1.09	1.01	0.73	1.69
0.2	10	1.63	0.46	0.86	1.09	1.01	0.73	1.69
0.25	12.5	1.62	0.46	0.86	1.09	1.01	0.73	1.69
0.5	25	1.62	0.46	0.85	1.08	1	0.72	1.68
0.75	37.5	1.6	0.45	0.84	1.07	0.99	0.72	1.67

1	50	1.29	0.37	0.68	0.87	0.8	0.58	1.35
2	100	1.52	0.43	0.8	1.02	0.94	0.68	1.58
3	150	1.47	0.42	0.77	0.98	0.91	0.66	1.53
4	200	1.41	0.4	0.75	0.95	0.88	0.63	1.47
5	250	1.36	0.39	0.72	0.91	0.85	0.61	1.42

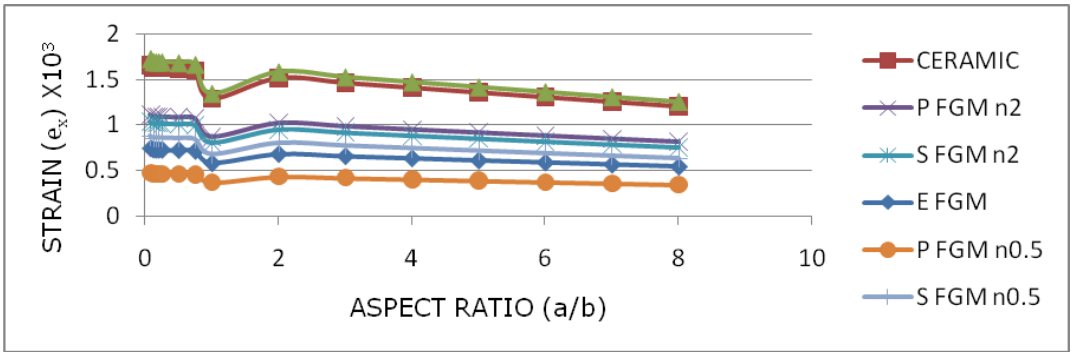

Figure 4: Strain ($e_x x10^3$) Under Constant Thermal Environment.

Shear Strain (e_{xy})

Table 5: Shear Strain (e_{xy} x1000) Under Constant Thermal Environment

a/b	a/h	Ceramic (n=0)	P-FGM-n 0.5	S-FGM-n 0.5	P-FGM-n2	S-FGM-n2	E-FGM	Metal (n=∞)
0.16	8	15.85	10.34	11.7	13.67	13.4	12	16.66
0.2	10	16.72	10.91	12.3	14.41	14.2	12.66	17.58
0.25	12.5	17.55	11.45	12.9	15.13	14.9	13.29	18.45
0.5	25	19.83	12.94	14.6	17.1	16.8	15.02	20.85
0.75	37.5	20.72	13.52	15.3	17.87	17.6	15.69	21.79
1	50	20.92	13.65	15.4	18.04	17.7	15.84	22
2	100	19.74	12.88	14.6	17.02	16.7	14.95	20.75
3	150	18.44	12.03	13.6	15.9	15.6	13.97	19.39
4	200	17.43	11.37	12.8	15.03	14.8	13.19	18.32
5	250	16.6	10.83	12.2	14.31	14.1	12.57	17.45

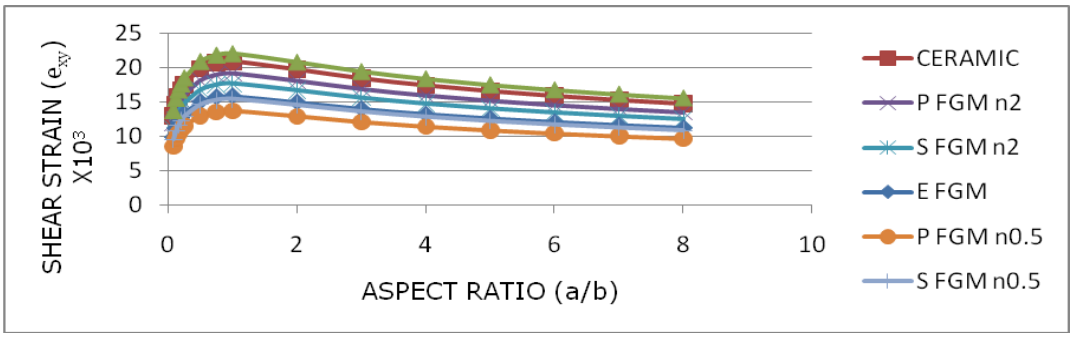

Figure 5: Shear Strain ($e_{xy} x10^3$) Under Constant Thermal Environment.

3.2 Effect of Aspect Ratio (A/B) In Constant Thermal Environment Under Mechanical Load

Non dimensional parameters are computed when the FGM plate is subjected to constant thermal environment of 100 °C and a constant udl of 1MPa for various values of aspect ratio (a/b). Non dimensional parameters are depicted in Tables 6,7,8,9 and 10. Graphical comparisons have presented in figures. 6,7,8,9 and 10.

The observations are as follows:

- Maximum deflection for P-FGM-n2 ($\overline{u_z}$ = 9.71) is found to be greater than that of S-FGM-n2 ($\overline{u_z}$ =9.27). Also deflection for P-FGM-n0.5 ($\overline{u_z}$ = 7.96) is found to be less than that of S-FGM-n0.5 ($\overline{u_z}$ =8.59) (table 6). The deflection shows increase up to aspect ratio 3 and constant nature afterwards (figure 6).
- Maximum tensile stress for P-FGM-n2 ($\overline{\sigma_x}$ = 534.5) is found to be greater than that of S-FGM-n2 ($\overline{\sigma_x}$=500.6). Also tensile stress for P-FGM-n0.5 ($\overline{\sigma_x}$ = 438.7) is found to be less than that of S-FGM-n0.5 ($\overline{\sigma_x}$ =475.2) (table 7). The tensile stress is showing sharp rise up to aspect ratio 1 and decrease afterwards (figure 7).
- Maximum shear stress for P-FGM-n2 ($\overline{\sigma_{xy}}$ = 874) is found to be greater than that of S-FGM-n2 ($\overline{\sigma_{xy}}$=842). Also shear stress in case of P-FGM-n0.5 ($\overline{\sigma_{xy}}$ = 779) is found to be less than that of S-FGM-n0.5 ($\overline{\sigma_{xy}}$ =815) (table 8). The shear stress is showing sharp rise upto aspect ratio 2 and constant nature afterwards (figure 8).
- Maximum strain (e_x) for P-FGM-n2 (e_x = 5.67) is found to be greater than that of S-FGM-n2 (e_x=5.31) (table 9). The strain is showing sharp rise up to aspect ratio 1 and sharp decline afterwards (figure 9).
- Maximum shear strain (e_{xy}) for P-FGM-n2 (e_{xy} = 32.38) is found to be greater than that of S-FGM-n2 (e_{xy}=31.13) (table 10). The shear strain is showing sharp rise up to aspect ratio 2 and constant nature afterwards (figure 10).
- Maximum deflection for E-FGM ($\overline{u_z}$ = 9.37) lies in between P-FGM-n2 ($\overline{u_z}$ = 9.71) and S-FGM-n 2 ($\overline{u_z}$ = 9.27). Similar trend is also observed in case of tensile stress, shear stress, strain and shear strain where the value of these parameters for E-FGM is found to be in between P-FGM n2 and P-FGM n0.5.

3.2.1 Non-Dimensional Deflection ($\overline{u_z}$)

Table 6: Non-Dimensional Deflection ($\overline{u_z}$) Under Constant Thermo Mechanical Load

a/b	a/h	Ceramic (n=0)	P-FGM-n 0.5	S-FGM-n 0.5	P-FGM-n2	S-FGM-n2	E-FGM	Metal (n=∞)
0.16	8	0.01	0.02	0.02	0.02	0.02	0.02	0.01
0.2	10	0.02	0.03	0.03	0.04	0.04	0.03	0.02
0.25	12.5	0.05	0.06	0.06	0.07	0.07	0.07	0.05
0.5	25	0.62	0.47	0.49	0.58	0.58	0.55	0.63
0.75	37.5	2.03	1.42	1.51	1.74	1.69	1.64	2.09
1	50	3.9	2.64	2.84	3.24	3.13	3.06	4.03
2	100	9.59	6.31	6.8	7.71	7.37	7.27	9.95
3	150	11.53	7.54	8.14	9.21	8.79	8.69	11.97
4	200	12.06	7.87	8.5	9.61	9.17	9.07	12.52
5	250	12.19	7.96	8.59	9.71	9.27	9.37	12.66

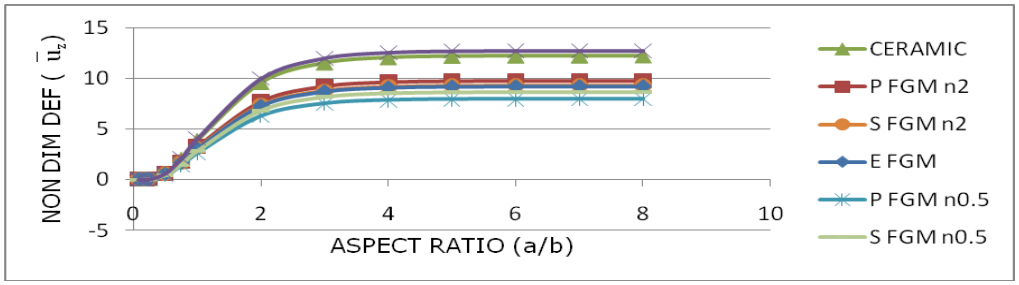

Figure 6: Non-Dimensional Deflection ($\overline{u_z}$) Under Constant Thermo Mechanical Load.

3.2.2 Non-Dimensional Tensile Stress ($\overline{\sigma_x}$)

Table 7: Non-Dimensional Tensile Stress ($\overline{\sigma_x}$) Under Thermo Mechanical Load

a/b	a/h	Ceramic (n=0)	P-FGM-n 0.5	S-FGM-n 0.5	P-FGM-n2	S-FGM-n2	E-FGM	Metal (n=∞)
0.16	8	18.4	13.2	29.7	64.4	53.6	32.2	17.5
0.2	10	75.7	33.1	50.5	86.4	74.6	53.4	71.9
0.25	12.5	21.7	63.2	82	119.9	106.5	85.4	120.6
0.5	25	200.5	247.2	274.6	323.7	300.7	281.9	190.5
0.75	37.5	343.1	383.5	417.3	474.2	443.6	428.4	325.9
1	50	400.8	438.7	475.2	534.5	500.6	488.8	380.7
2	100	339.7	375	408.4	462.3	431.2	423.1	322.7
3	150	324.4	358.6	391.2	444.2	414.1	405.5	308.2
4	200	323.3	357.2	389.8	442.8	412.7	404.1	307.2
5	250	322	356.7	389.2	442.3	412.3	403.7	305.9

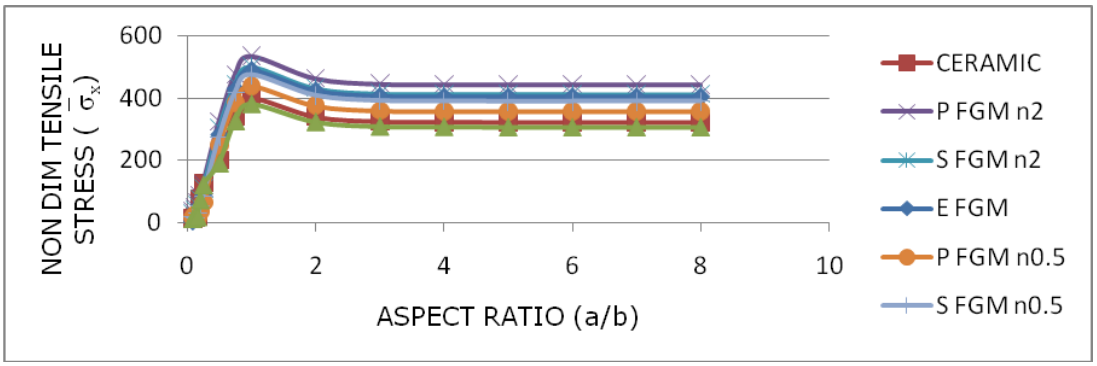

Figure 7: Non-Dimensional Tensile Stress ($\overline{\sigma_x}$) Under Thermo Mechanical Load.

3.2.3 Non-Dimensional Shear Stress ($\overline{\sigma_{xy}}$)

Table 8: Non-Dimensional Shear Stress ($\overline{\sigma_{xy}}$) Under Constant Thermo Mechanical Load

a/b	a/h	Ceramic (n=0)	P-FGM-n 0.5	S-FGM-n 0.5	P-FGM-n2	S-FGM-n2	E-FGM	Metal (n=∞)
0.16	8	294	334	377	392	360	329	279
0.2	10	308	350	396	414	381	348	293
0.25	12.5	321	363	412	436	402	367	305
0.5	25	334	417	455	512	475	435	317
0.75	37.5	435	515	540	582	562	531	413
1	50	545	635	665	714	689	658	517
2	100	674	769	805	863	828	803	640
3	150	668	768	804	862	830	800	635
4	200	672	776	812	871	840	807	638
5	250	676	779	815	874	842	810	642

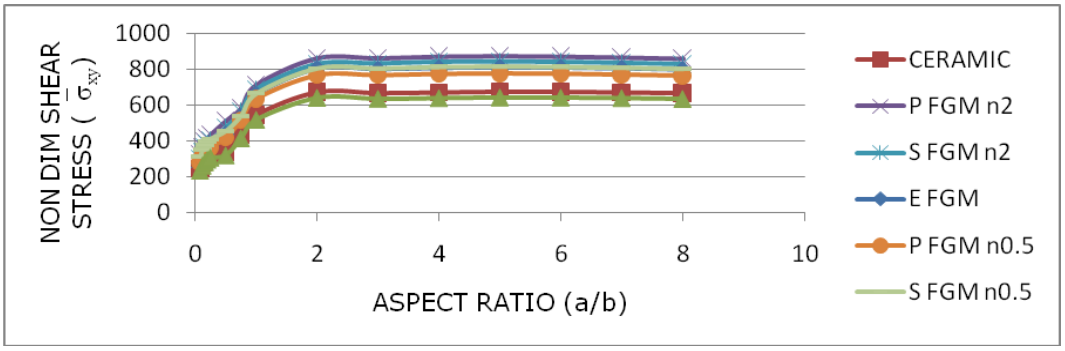

Figure 8: Non-Dimensional Shear Stress ($\bar{\sigma}_{xy}$) Under Constant Thermo Mechanical Load.

3.2.4 Strain (e_x)

Table 9: Strain (e_x x10^3)Under Constant Thermo Mechanical Load

a/b	a/h	Ceramic (n=0)	P-FGM-n 0.5	S-FGM-n 0.5	P-FGM-n2	S-FGM-n2	E-FGM	Metal (n=∞)
0.16	8	1.36	0.79	1.01	1.52	1.38	0.72	1.31
0.2	10	1.7	1.02	1.25	1.81	1.65	0.87	1.66
0.25	12.5	2.21	1.35	1.62	2.24	2.06	1.08	2.18
0.5	25	5.05	3.2	3.63	4.57	4.28	1.35	5.12
0.75	37.5	6.52	4.08	4.58	5.67	5.31	1.75	6.66
1	50	6.3	3.83	4.31	5.33	4.98	3.96	6.46
2	100	3.95	2.3	2.64	3.39	3.14	5.04	4.05
3	150	3.74	2.16	2.49	3.23	2.98	4.77	3.82
4	200	3.71	2.14	2.47	3.19	2.95	2.94	3.79
5	250	3.7	2.12	2.45	3.17	2.93	2.78	3.78

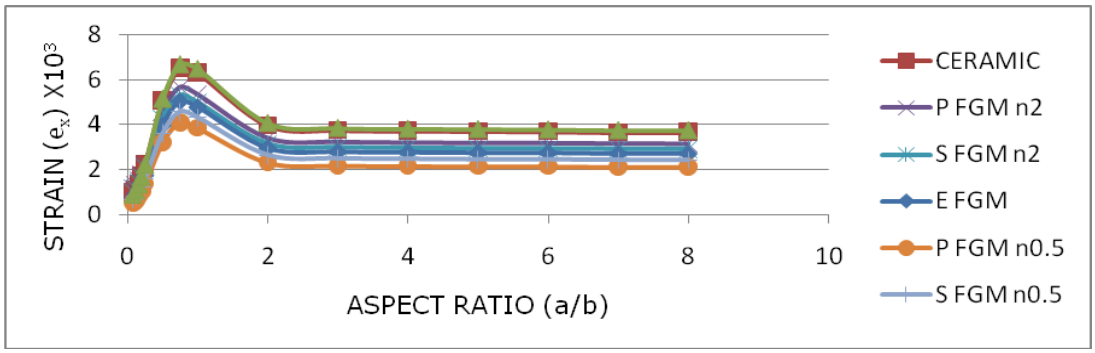

Figure 9: Strain (e_x x10^3) Under Constant Thermo Mechanical Load.

3.2.5 Shear Strain (e_{xy})

Table 10: Shear Strain (e_{xy}x10^3)Under Constant Thermo Mechanical Load

a/b	a/h	Ceramic (n=0)	P-FGM-n 0.5	S-FGM-n 0.5	P-FGM-n2	S-FGM-n2	E-FGM	Metal (n=∞)
0.16	8	13.33	10.19	11.64	14.52	13.32	12	12.93
0.2	10	14.09	10.78	12.3	15.34	14.09	12.66	13.66
0.25	12.5	14.85	11.37	12.97	16.15	14.85	13.29	14.41
0.5	25	17.66	13.54	15.34	18.96	17.56	15.02	17.23
0.75	37.5	22.26	16.72	18.19	21.58	20.77	15.69	22.37
1	50	27.95	20.61	22.39	26.45	25.46	15.84	28.22
2	100	34.94	24.95	27.13	31.97	30.6	14.95	35.43
3	150	34.47	24.93	27.1	31.94	30.7	13.97	34.94

4	200	34.62	25.18	27.37	32.28	31.05	13.19	35.07
5	250	34.86	25.27	27.47	32.38	31.13	12.57	35.33

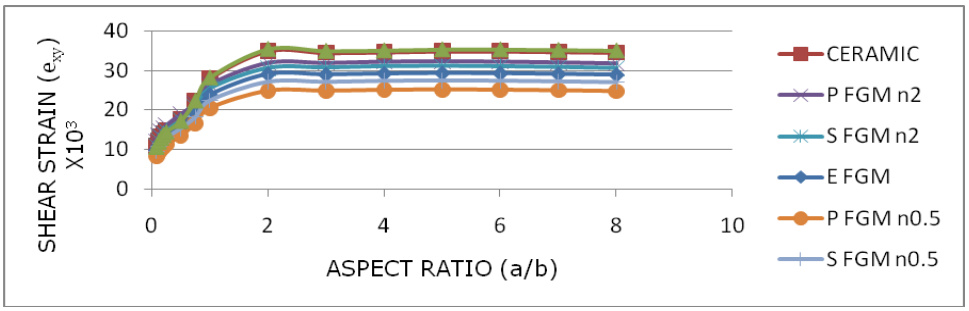

Figure 10: Shear Strain ($e_{xy}x10^3$) Under Constant Thermo Mechanical Load.

4. CONCLUSIONS

An FGM plate made of ceramic and metal has been studied under thermal and thermomechanical environment. Parametric study has been performed by material distribution and temperature. The following conclusions are drawn:

- Deflection for FGM plates (i.e. 0<n<∝) are lesser than that of metal plate. Tensile stress is least for ceramic and metal as compared to various FGMs. The tensile stress in the metal rich region is comparable to that in the ceramic rich region. As volume fraction index increases shear stress diverges and gives clear trends.
- P-FGM (n=0.5) plate depicts the least deflection, strain and stress among all FGMs. The reason is attributed that the stiffness of the P-FGM (n=0.5) plate is higher than that of E-FGM plate and stiffness of the E-FGM plate is higher than that of P-FGM (n=2).

The work may be extended to study FG plates more complex mechanisms such as variable mechanical and thermal loading combinations.

REFERENCES

1. *Woo YL, David PS, Christopher CB, Fazil E, Yi-DL, Zaher M. (1996). Concept of Functionally Graded Materials for Advanced Thermal Barrier Coating Applications. J Am. Ceram,79: 3003-3012.*
2. *J.N. Reddy and Q.C. Zhen. (2001). Three-Dimensional Thermo mechanical Deformations of Functionally Graded Rectangular Plates. Eur. J Mech. A/Solids. 20:841–855.*
3. *W. Hui and Q. Qing-Hua. (2008). Meshless Approach for Thermo-Mechanical Analysis of Functionally Graded Materials," Engg. Analysis with Boundary Elements. 32:704–712.*
4. *Duc ND, Tung HV. (2010). Mechanical and Thermal Post buckling Of Shear-Deformable FGM Plates with Temperature-Dependent Properties. Mechanics of Composite Materials. 46: 461-476.*
5. *R. Xiaohui and W. Zhen. (2018). A refined sinusoidal model for functionally graded plates subjected to thermomechanical loading. Journal of Composite Materials. https://doi.org/10.1177/0021998318814158, 2018.*
6. *K. Sai Priyanka, Babitha Kodavanla, A. Barai & N. Madhavi, "Thermo-Mechanical Analysis of High Temperature Insulating Composites", IJMPERD, Vol. 8, Issue 3, pp. 915-920*
7. *Jawad K. Zeboon, "Analytical Analysis for Simply Supported Composite Plates Under Uniformly Distributed Load", International Journal of General Engineering and Technology (IJGET), Vol. 6, Issue5, pp. 17-24*

8. *Osama Mohamed Irfan, "Influence of Specimen Geometry and Lubrication Conditions on the Compression behavior of Aa6066 Aluminum Alloy", International Journal of Mechanical Engineering (IJME), Vol. 5, Issue 1, pp. 14-24*
9. *Aravind Tripathy, Saroj Kumar Sarangi & Rashmikant Panda, "Fabrication of Functionally Graded Composite Material using Powder Metallurgy Route: An Overview", IJMPERD, Vol. 7, Issue 6, pp. 135-146*